



Iron complexes of tris(pyrazolyl)ethane ligands methylated in the 3-, 4-, and 5-positions



Margaret A. Goodman^a, Michael J. DeMarco^b, Steven E. Tarasek^b, Alexander Y. Nazarenko^c, William Brennessel^d, M. Scott Goodman^{c,*}

^a Department of Math and Natural Sciences, D'Youville College, Buffalo, NY 14201, USA

^b Department of Physics, SUNY Buffalo State, Buffalo, NY 14222, USA

^c Department of Chemistry, SUNY Buffalo State, Buffalo, NY 14222, USA

^d Department of Chemistry, University of Rochester, Rochester, NY 14627, USA

ARTICLE INFO

Article history:

Received 2 June 2014

Received in revised form 12 August 2014

Accepted 16 August 2014

Available online 6 September 2014

Keywords:

Tris(pyrazolyl)ethane

Tris(pyrazolyl)methane

Spin crossover

Iron complexes

Mössbauer spectroscopy

ABSTRACT

Four tris(pyrazolyl)ethane (tpe) ligands were synthesized from tris(pyrazolyl)methane (tpm) starting materials. The new tpe ligands differ only in the placement of methyl groups on the pyrazole rings. For each tpe ligand, the 2:1 complex with Fe(II) was readily synthesized and the structures were determined by X-ray crystallography and characterized more completely by ⁵⁷Fe Mössbauer spectroscopy, ¹H NMR, and UV–Vis spectroscopy. The complexes all contain Fe(II) in the low spin (LS) state at low temperatures, but differ in Fe–N bond lengths and spectroscopic parameters. Methyl groups in the 5-position of the pyrazoles of the tpe ligand close the bite of the ligand, strengthening the ligand field and shifting the visible absorbance band of the complex to higher energies. Methyls in the 4-position had almost no effect on the ligand, making the iron(II) complex almost indistinguishable from that of the parent tpe ligand. Methyl groups in the 3-position of the tpe ligand cause an opening of the bite of the ligand, which is evidenced by increased Fe–N bond lengths in the complex and a shift of the visible absorbance to lower energies. The complex with methyls in the 3-position also starts to display spin crossover behavior near room temperature, whereas the other tpe complexes do not.

© 2014 Elsevier B.V. All rights reserved.

1. Introduction

The tris(pyrazolyl)borates (tp) and tris(pyrazolyl)methanes (tpm) are tripodal, nitrogen-donor ligands that readily form complexes with numerous metal ions [1,2]. These ligands, sometimes also referred to as “scorpionates”, consist of a central atom, either boron (tp) or carbon (tpm), bonded to each of three pyrazole moieties through one nitrogen atom of the pyrazole rings, which leaves the second nitrogen of each pyrazole available for chelating to a metal ion (Fig. 1). With metal ions such as Fe(II), these ligands generally form pseudo-octahedral complexes containing two ligands, provided that the substituents in the 3-position of the pyrazoles (R₁ in Fig. 1) are not so bulky as to prevent inter-digitation of these groups in the complex [2d].

Since Fe(II) has a 3d⁶ electronic configuration, octahedral complexes of Fe(II) can have either a high-spin (HS, S = 2) or a low-spin (LS, S = 0) ground-state electronic configuration. The ligand field strength of tpm ligand is poised so that Fe(II) complexes can some-

times exhibit temperature-dependent spin crossover (SCO) behavior induced by temperature, irradiation, or pressure in the solid state or in solution [2,3]. In the case of temperature-induced SCO transitions, the change between the diamagnetic LS state and the paramagnetic HS state can occur gradually or abruptly, with the transition temperature being dependent on the nature of the substituents on the N-donor heterocycles [4].

Chemical modification of the central carbon atom of tpm and related ligands can be achieved by deprotonation with a strong base followed by treatment with an electrophile [5]. Perhaps the simplest modification of the central carbon is the introduction of a methyl group to afford a 1,1,1-tris(pyrazolyl)ethane ligand (tpe) (Fig. 1). A few examples of metal complexes containing the unsubstituted tpe ligand have been reported previously [5b,6]. More elaborate functionalization of the tpm carbon has been employed by Reger for the creation of a number of functionalized tpm ligands that form fascinating supramolecular structures when complexed to metal ions [7].

As a result of our interest in the chemistry of tpm complexes that exhibit spin-state transitions near room temperature [8], we undertook the synthesis and study of a simple series of tpe ligands

* Corresponding author. Tel.: +1 (716) 878 5204.

E-mail address: goodmams@buffalostate.edu (M.S. Goodman).

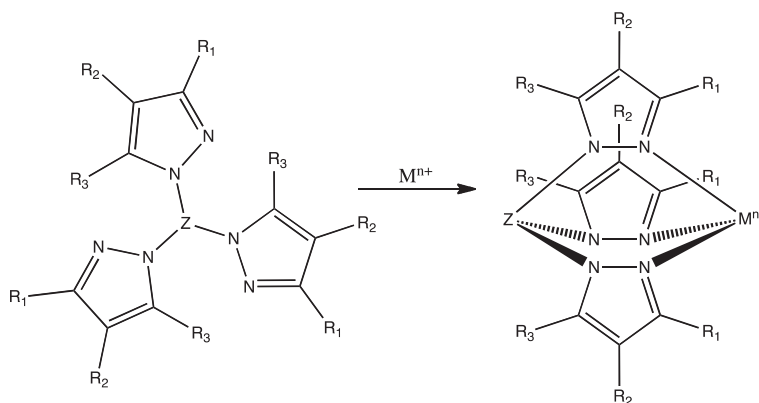


Fig. 1. The tris(pyrazolyl)borates ($Z = BH^-$), methanes ($Z = CH$), and ethanes ($Z = CCH_3$) with substituents R_1 , R_2 , and R_3 .

with methyls on the pyrazole rings (Fig. 2). For simplicity, the tpe ligands are denoted with a superscript indicating where the methyl groups are located on the pyrazole rings (e.g. tpe^{3Me} has a methyl group in the 3-position of each pyrazole). These substituted tpe ligands were then allowed to complex with Fe(II) and the properties of these complexes are reported. The numbering system for the Fe(II) complexes is analogous to that of the ligands. For example, complex 4 is the Fe(II) complex of tpe^{4Me} , which has methyl groups in the 4-positions of the pyrazoles. The results of our efforts once again show that the steric environment of tris-pyrazole ligands can cause large differences in the structural and electronic properties of the corresponding Fe(II) complexes.

2. Experimental

2.1. General

All solvents were reagent grade and used without further purification, except toluene, which was distilled from Na, and THF, which was distilled from Na/K alloy. Iodomethane, butyllithium solution, 3-methylpyrazole and iron(II) tetrafluoroborate hexahydrate were purchased from Acros Organics and used without further purification. 1,1,1-tris(pyrazolyl)ethane (tpe) [5a] and tris(4-methylpyrazolyl)methane (tpe^{4Me}) [9] were synthesized according to literature procedures.

FT-IR spectra were recorded on a Thermo Nexus 470 equipped with a diamond ATR. 1H and ^{13}C NMR spectra were recorded on a Bruker Avance 300 MHz NMR or a Bruker Avance III 400 MHz instrument. Low-resolution mass spectra were recorded on a Thermo Finnigan Trace-DSQ GC/MS instrument with EI ionization. High resolution mass spectra were recorded on a Thermo Exactive with a ESI source. UV-Vis spectra and reflectance spectra were recorded on a Shimadzu UV-2600.

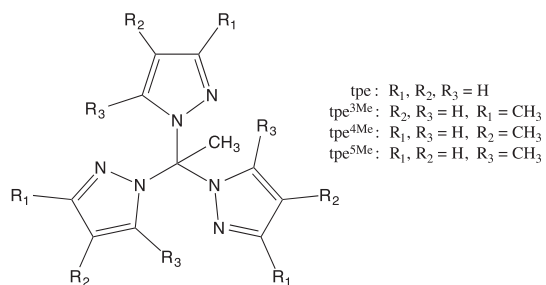


Fig. 2. The methylated tris(pyrazolyl)ethane (tpe) ligands used in this study.

2.2. Synthesis of 1,1,1-tris(5-methylpyrazolyl)ethane (tpe^{5Me})

This ligand was prepared by a method previously reported for producing tris(5-methylpyrazolyl)methane [8].

A solution of **1** (0.34 g/1.5 mmol) in THF (15 mL) was cooled to between -30 and -40 °C (dry ice/acetonitrile bath) under argon. To the cooled solution was carefully added *n*-butyllithium (2.4 mL/6 mmol, 2.5 M in hexanes, 4 eq.). The resulting mixture was stirred for 1 h at -30 °C, and then cooled to -78 °C in a dry ice/acetone bath. Iodomethane (0.37 mL/6 mmol, 4 eq.) was slowly added and stirring was continued at -78 °C for 1 h after addition was completed. The cold bath was removed and the reaction mixture was allowed to warm to room temperature over 2 h. The reaction was carefully quenched by the addition of a small amount of methanol, the volatiles were removed by rotary evaporation, and the resulting material was dissolved in CH_2Cl_2 (25 mL) and washed twice with water (10 mL) to remove excess lithium salts. The CH_2Cl_2 layer was dried with Na_2SO_4 and evaporated. Pure tpe^{5Me} was obtained by crystallization of the residue from toluene/hexanes (1:1). Yield: 0.14 g (35% yield); mp: 123 – 124 °C; *Anal. Calc.* for $C_{14}H_{18}N_6$: C, 62.20; H, 6.71; N, 31.09. Found: C, 62.27; H, 6.82; N, 31.35%. 1H NMR ($CDCl_3$) δ 7.46 (d, $J = 1.5$ Hz, 3H), 6.14 (d, $J = 0.6$ Hz, 3H), 2.89 (s, 3H), 1.91 (s, 9H); ^{13}C NMR ($CDCl_3$) δ 141.3, 138.9, 109.4, 91.9, 30.4, 12.6; IR (diamond ATR, cm^{-1}) 3125, 2940, 1548, 1464, 1456, 1349, 1245, 1211, 919, 796. HRMS: ESI(+) (m/z) calcd. for $[C_{14}H_{18}N_6Na]^+$ 293.1485, found 293.1487.

2.3. Synthesis of 1,1,1-tris(4-methylpyrazolyl)ethane (tpe^{4Me})

Tris(4-methylpyrazolyl)methane (1.153 g., 1.5 mmol) was dissolved in dry THF (25.0 mL) and was cooled to -78 °C under argon. To the cooled solution was added *n*-butyllithium (1.6 M in hexanes, 3.4 mL, 5.4 mmol, 1.2 eq.). The resulting mixture was stirred at this temperature for 1 h, and then iodomethane (0.34 mL, 5.4 mmol, 1.2 eq.) was added and stirring was continued at -78 °C for 1 h. The cooling bath was removed and the reaction mixture was allowed to warm to room temperature over 2 h. The reaction was carefully quenched by the addition of a small amount of methanol, and the THF was then removed by rotary evaporation. The crude residue was taken up in methylene chloride (50 mL) and extracted twice with water (25 mL). The organic portion was dried (Na_2SO_4) and evaporated to a colorless oily solid. Pure tpe^{4Me} was obtained by crystallization of the residue from diethyl ether. Yield: 0.546 g (45% yield); mp: 130 – 131 °C. *Anal. Calc.* for $C_{14}H_{18}N_6$: C, 62.20; H, 6.71; N, 31.09. Found: C, 62.20; H, 6.74; N, 31.13%. 1H NMR ($CDCl_3$) δ 7.48 (s, 3H), 6.60 (d, $J = 0.6$ Hz, 3H), 2.86 (s, 3H), 2.04 (s, 9H); ^{13}C NMR ($CDCl_3$) δ 142.7, 128.2, 117.8, 90.5, 26.9, 9.60; IR (diamond ATR, cm^{-1}) 2940, 1548, 1390, 1350, 1270, 1179, 1013, 963, 861,

788. HRMS: ESI(+) (m/z) calcd. for $[C_{14}H_{18}N_6Na]^+$ 293.1485, found 293.1484.

2.4. Synthesis of 1,1,1-tris(3-methylpyrazolyl)ethane (tpe^{3Me})

To a solution of 3-methylpyrazole (4.024 g/50 mmol) and tetrabutylammonium bromide (0.806 g/2.5 mmol) in 50 mL of H_2O , sodium carbonate (31.797 g/0.3 mol) was added gradually. The reaction was allowed to cool to room temperature, chloroform (25 mL) was added, and the solution was heated at reflux. At the end of 3 days, excess sodium carbonate was filtered off, the dark chloroform layer was separated, and the aqueous phase was extracted 3 times with diethyl ether (25 mL). The combined organic portions were dried (Na_2SO_4) and evaporated to an oily solid. NMR of the crude product indicated the presence of all four possible regioisomers of tris(3-methylpyrazolyl)methane (see [Supplementary data](#)).

The regioisomeric mixture from above was dissolved in a mixture of dry toluene (75 mL) and *p*-toluene sulfonic acid (0.025 g/0.15 mmol). The solution was heated at reflux for 24 h under nitrogen and then allowed to cool to room temperature. Dichloromethane (200 mL) was added and the organic mixture was washed 3 times with a saturated sodium bicarbonate solution (20 mL). The organic phase was decolorized with charcoal and then dried with Na_2SO_4 . Rotary evaporation of the volatiles resulted in a yellow oil. NMR of this material indicated the presence of mainly two regioisomers, tris(3-methylpyrazolyl)methane and the bis(3-methylpyrazolyl)(5-methylpyrazolyl)methane, in an approximate 2:1 ratio. The other two regioisomers tris(5-methylpyrazolyl)methane and the bis(5-methylpyrazolyl)(3-methylpyrazolyl)methane represent <10% of the mixture (see [Supplementary data](#)). Crude yield 3.502 g. (82%).

A portion of the crude mixture of two regioisomers from the previous reaction (1.281 g/5.0 mmol) was dissolved in dry THF (15 mL) and was cooled to $-78^\circ C$ under argon. To the cooled solution was added *n*-butyllithium (1.6 M in hexanes, 3.8 mL, 6.0 mmol, 1.2 eq.). The resulting mixture was stirred at this temperature for 30 minutes, and then iodomethane (0.38 mL/6.0 mmol, 1.2 eq.) was added and stirring was continued at $-78^\circ C$ for 1 h. The cooling bath was removed and the reaction mixture was allowed to warm to room temperature over 2 h. The reaction was carefully quenched by the addition of a small amount of methanol, and the THF was then removed by rotary evaporation. The crude residue was taken up in methylene chloride (25 mL) and extracted twice with water (15 mL). The organic portion was dried (Na_2SO_4) and evaporated to a colorless oily solid. NMR of this material indicated the presence of mainly two regioisomers, tris(3-methylpyrazolyl)ethane and the bis(3-methylpyrazolyl)(5-methylpyrazolyl)ethane, in an approximate 2:1 ratio (see [Supplementary data](#)).

The regioisomeric mixture of *tpe* compounds from above was dissolved in a mixture of dry toluene (40 mL) and *p*-toluene sulfonic acid (0.020 g/0.12 mmol). The solution was heated at reflux for 24 h under nitrogen and then allowed to cool to room temperature. Dichloromethane (200 mL) was added and the mixture was washed with a saturated sodium bicarbonate solution (3×20 mL). The organic layer was decolorized with charcoal, filtered and dried with Na_2SO_4 . Evaporation of the volatiles resulted in a white solid. Pure tpe^{3Me} was obtained by crystallization of the residue from diethyl ether to afford 0.510 g (42%), mp: 137–139 $^\circ C$. *Anal.* Calc. for $C_{14}H_{18}N_6$: C, 62.20; H, 6.71; N, 31.09. Found: C, 62.53; H, 6.78; N, 30.68%. 1H NMR ($CDCl_3$) δ 6.58 (d, $J = 2.7$ Hz, 3H), 6.06 (d, $J = 2.4$ Hz, 3H), 2.88 (s, 3H), 2.29 (s, 9H); ^{13}C NMR ($CDCl_3$) δ 151.0, 130.0, 106.7, 90.0, 26.4, 14.1; IR (diamond ATR, cm^{-1}) 3126, 2927, 1527, 1455, 1389, 1377, 1357, 1261, 1204, 1042, 967, 792. HRMS: ESI(+) (m/z) calcd. for $[C_{14}H_{18}N_6Na]^+$ 293.1485, found 293.1486.

2.5. Preparation of Fe(II) complexes (**1**, **3**–**5**)

Complexes of the various *tpe* ligands with Fe(II) were prepared with the following procedure. All glassware was dried for 30 min. in an $80^\circ C$ oven before use and flushed with argon. The corresponding tris(pyrazolyl)ethane ligand (1.00 mmol) was dissolved in dry THF (4 mL) under argon. In a separate flask, iron(II) tetrafluoroborate hexahydrate (0.168 g, 0.50 mmol) was dissolved in dry THF (1 mL) under argon. The *tpe* solution was then added to the Fe(II) solution via syringe, and the mixture was stirred for 1 h at room temperature. The products, all fine powders, were isolated by filtration, rinsed with fresh THF, and allowed to air-dry. The compounds could each be crystallized by vapor diffusion of ether into an acetonitrile solution at $-30^\circ C$.

2.5.1. $[Fe(tpe)_2]^{2+} \cdot 2BF_4^-$ (**1**)

1H NMR (CD_3CN) δ 8.54 (dd, $J = 2.8$, 0.4 Hz, 6H), 7.26 (d, $J = 1.6$ Hz, 6H), 6.56 (dd, $J = 2.8$, 0.4 Hz, 6H), 3.47 (s, 6H); ^{13}C NMR (CD_3CN) δ 151.0, 135.9, 110.2, 84.3, 20.9; IR (diamond ATR, cm^{-1}) 3160, 1418, 1398, 1328, 1236, 1123, 1088, 983, 741, 604. HRMS: ESI(+) (m/z) calcd. for $[C_{22}H_{24}N_{12}FeBF_4]^+$ 599.1620, found 599.1625.

2.5.2. $[Fe(tpe^{3Me})_2]^{2+} \cdot 2BF_4^-$ (**3**)

1H NMR (CD_3CN) δ 16.7 (s, 6H), 7.49 (s, 18H), 7.21 (s, 6H), -0.65 (s, 6H); ^{13}C NMR (CD_3CN) δ 151.4, 131.1, 118.4, 107.4, 26.7, 13.9; IR (diamond ATR, cm^{-1}) 3632, 3572, 3148, 1531, 1394, 1228, 1082, 1034, 769. *Anal.* Calc. for $C_{28}H_{36}N_{12}FeB_2F_8$: C, 43.67; H, 4.71; N, 21.83. Found: C, 43.76; H, 4.74; N, 21.87%. HRMS: ESI(+) (m/z) calcd. for $[C_{28}H_{36}N_{12}FeBF_4]^+$ 683.2559, found 683.2557.

2.5.3. $[Fe(tpe^{4Me})_2]^{2+} \cdot 2BF_4^-$ (**4**)

1H NMR (CD_3CN) δ 8.28 (s, 6H), 7.03 (s, 6H), 3.29 (s, 6H), 2.18 (s, 18H); ^{13}C NMR (CD_3CN) δ 151.6, 134.1, 121.1, 84.0, 21.0, 9.3; IR (diamond ATR, cm^{-1}) 3136, 1394, 1351, 1204, 1166, 1034, 845, 782. *Anal.* Calc. for $C_{28}H_{36}N_{12}FeB_2F_8 \cdot 2H_2O$: C, 41.72; H, 5.00; N, 20.85. Found: C, 41.94; H, 5.01; N, 20.65%. HRMS: ESI(+) (m/z) calcd. for $[C_{28}H_{36}N_{12}FeBF_4]^+$ 683.2559, found 683.2563.

2.5.4. $[Fe(tpe^{5Me})_2]^{2+} \cdot 2BF_4^-$ (**5**)

1H NMR (CD_3CN) δ 6.98 (s, 6H), 6.27 (s, 6H), 3.40 (s, 6H), 2.80 (s, 18H); ^{13}C NMR (CD_3CN) δ 149.2, 148.7, 113.2, 91.2, 24.1, 18.0; IR (diamond ATR, cm^{-1}) 3366, 3149, 1564, 1479, 1392, 1220, 1026, 956, 807, 774. *Anal.* Calc. for $C_{28}H_{36}N_{12}FeB_2F_8 \cdot CH_3CN$: C, 44.50; H, 4.87; N, 22.32. Found: C, 44.42; H, 4.85; N, 22.45%. HRMS: ESI(+) (m/z) calcd. for $[C_{28}H_{36}N_{12}FeBF_4]^+$ 683.2559, found 683.2562.

2.5.5. Synthesis of complex **3** by thermal rearrangement of **5**

A solution of **5** (30 mg/0.037 mmol) in d_3 -acetonitrile (2.0 mL) was refluxed under Argon. Periodically, 1H NMR spectra were taken to judge the progress of the reaction. When the reaction was deemed to be finished, about 24 h, the solution was cooled and allowed to slowly evaporate. After sufficient concentration, dark purple crystals of compound **3** were deposited and found to be identical to an authentic sample prepared from tpe^{3Me} as in Section 2.5.2.

2.6. X-ray crystallography

Initial evaluation of the crystal, unit cell determination, and X-ray intensity data measurement were performed using a Bruker SMART APEX II CCD or a Bruker D8 QUEST diffractometer. Crystals were mounted onto the tip of a 0.1 mm diameter glass fiber or a Mitigen MicroLoop for data collection at the desired temperature. The data collection was carried out using Mo $K\alpha$ radiation (graphite monochromator). A randomly oriented region of reciprocal

space was surveyed: three major sections of frames were collected with 0.50° steps in ω at three different φ settings and a detector position of -38° in 2θ . The intensity data were corrected for absorption [10]. Space groups were determined based on systematic absences and intensity statistics and the structures were solved using SIR97 [11] (or SHELXT [12]) and refined using SHELXL-97 [12]. A direct-methods solution was calculated, which provided most non-hydrogen atoms from the E-map. Full-matrix least squares/difference Fourier cycles were then performed, which located the remaining non-hydrogen atoms. All non-hydrogen atoms were refined with anisotropic displacement parameters. All hydrogen atoms were placed in ideal positions and refined as riding atoms with relative isotropic displacement parameters.

2.7. Mössbauer spectroscopy

The Mössbauer experiments on the Fe(II) complexes **1** and **3-5** were performed in vertical transmission geometry. The velocity calibration was performed with an α -Fe foil and isomer shifts are referenced to the foil for both of the experimental arrangements. The delrin sample holder contained less than 0.2 mg/cm^2 of ^{57}Fe for all the samples measured. Experiments at 298 K and below were performed inside the sample chamber of a Janis cryostat with the source, $^{57}\text{Co}(\text{Rh})$, 1 cm above the sample holder, which were both held at the same temperature in an air bath [13]. At 78 K the air bath was at a pressure lower than 40×10^{-2} mbar. The Mössbauer γ -ray was detected by a proportional counter placed below the cryostat mylar window. Data for each sample was first collected at 78 K and then warmed to room temperature, 298 K, for data collection at this temperature. Experiments at temperatures higher than 298 K (complex **3** only) were performed in air outside the cryostat using the same vertical geometry. In this case

the Mössbauer drive system with the sample a centimeter below the source was hung above the proportional counter detector. The sample was heated in air by a heater wire attached to the brass holder that in turn held the delrin sample holder. The sample plus source were allowed to reach thermal equilibrium before the experiments were commenced. The temperature was controlled by a Lakeshore temperature controller (300 series).

3. Results

3.1. Synthesis and structures

3.1.1. The Fe(II) complex of tpe (**1**)

Although the unsubstituted tpe ligand is known, the Fe(II) complex has not been previously described in detail. When two equivalents of tpe are added to one equivalent of $\text{Fe}(\text{BF}_4)_2 \cdot 6\text{H}_2\text{O}$ in THF, the rose-colored Fe(II) complex, $[\text{Fe}(\text{tpe})_2]^{2+} \cdot 2\text{BF}_4^-$ (**1**) precipitates almost instantly. It is well-known that LS Fe(II) complexes of tpm ligands are colored, typically violet, and HS complexes are colorless, thus the rose color of the solid complex immediately suggests a LS electronic structure. ^1H NMR spectra support this finding, as the signals are sharp and not significantly shifted from their expected frequencies.

Crystals of **1** suitable for X-ray diffraction can be readily grown by slow evaporation of an acetonitrile solution. The X-ray structure of the complex determined at 100 K is shown in Fig. 3. The symmetry of the complex in the crystal (space group = $C2/c$) results in three different Fe–N bond lengths, all close to 1.95 Å. These bond lengths are slightly shorter than those in the corresponding Fe–tpm complex (~ 1.97 Å), but are otherwise typical of LS Fe(II) complexes of this type – HS complexes typically have Fe–N bonds about 0.2 Å longer [14].

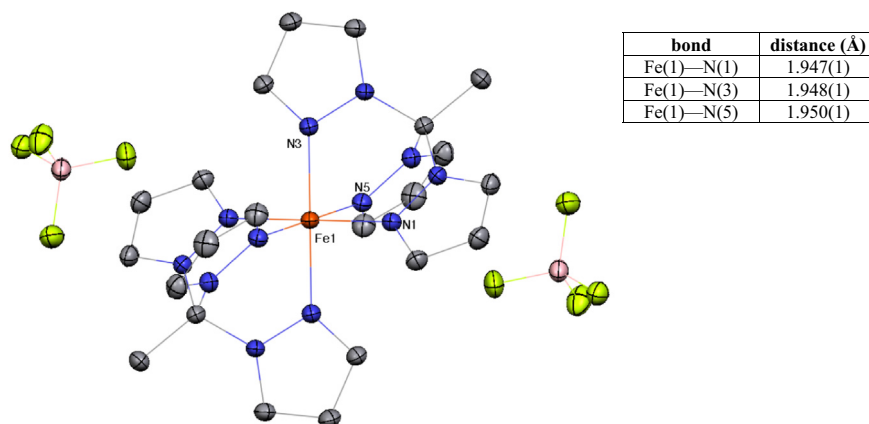


Fig. 3. Crystal structure of **1** at 100 K. Solvent molecules are not shown and hydrogen atoms have been omitted for clarity.

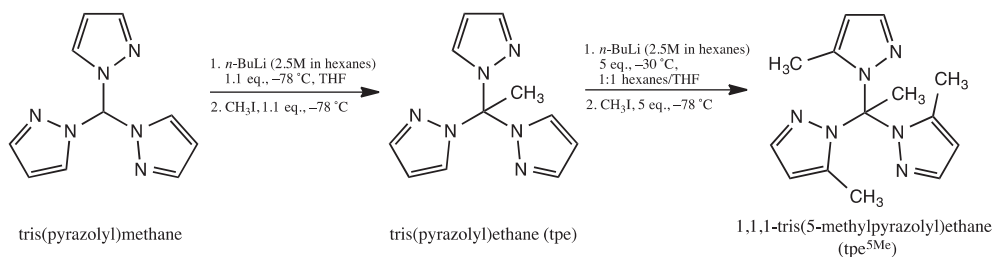


Fig. 4. The synthesis of 1,1,1-tris(5-methylpyrazolyl)ethane (tpe^{5Me}).

3.1.2. 1,1,1-tris(5-methylpyrazolyl)ethane (tpe^{5Me}) and its Fe(II) complex (**5**)

In a previous study [5a], Reger surmised that substituents on the 5-position of the pyrazole rings of tpm ligands render the deprotonated methine carbon unreactive towards electrophiles, other than a proton, due to steric hindrance. Our attempts at direct methylation of the methine carbon of the previously reported tris(5-methylpyrazolyl)methane [8] support that conclusion, as do the studies of Breher on the anion of tris(3,5-dimethylpyrazolyl)methane [15]. Therefore, an alternative synthetic approach to ligand **5** had to be devised, wherein the order of the methylation steps was simply reversed. Methylation of the methine carbon of the unsubstituted tris(pyrazolyl)methane was carried out first to produce tpe, followed by methylation in the three 5-positions to afford 1,1,1-tris(5-methylpyrazolyl)ethane (tpe^{5Me}) (Fig. 4).

Unexpectedly, when two equivalents of tpe^{5Me} are treated with 1 equivalent of Fe(II), the complex that precipitates from THF is not rose or violet, but rather a bright orange color. The 1H NMR spectrum of this material is sharp and shows only a single set of resonances attributable to the tpe ligand, completely consistent with this being a LS octahedral complex. A crystal of $[Fe(tpe^{5Me})_2]^{2+} \cdot 2BF_4^-$ (**5**) was subjected to X-ray analysis at 100 K, the result of which is shown in Fig. 5. As seen in the X-ray structure, the orange complex is indeed the expected octahedral, 2:1 complex. The symmetry of the complex in the crystal (space group = $P2_1/n$) again results in three different Fe–N bond lengths, all near 1.93 or 1.94 Å. Significantly, these are the shortest Fe–N bonds known in complexes of this type and clearly indicative of a LS Fe(II) complex.

3.1.3. 1,1,1-tris(4-methylpyrazolyl)ethane (tpe^{4Me}) and its Fe(II) complex (**4**)

The synthesis of tpe^{4Me} was carried out by methylation of the methine carbon of the corresponding tris(4-methylpyrazolyl)methane using standard procedures [5] (Fig. 6).

The Fe(II) complex **4** was again rose colored, indistinguishable from the color of complex **1**, and the 1H NMR spectrum was as expected for a LS complex. Crystals of this material suitable for X-ray structure determination proved difficult to grow, but were eventually grown from slowly evaporating mixture of acetonitrile and toluene. The X-ray structure determined at 100 K is shown in Fig. 7. The crystal (space group = $P4_2/mbc$) contains a $[Fe(tpe^{4Me})_2]^{2+}$ complex ion, and BF_4^- and solvent toluene groups that alternatively occupy positions next to a two-fold rotation axis (tetrafluoroborate) and mirror plane (toluene). The Fe–N bond lengths in this complex are almost identical: 1.9483(13) Å (Fe–N1) and 1.947(2) Å (Fe–N3). Taken together, the Fe–N bond lengths, the 1H and ^{13}C NMR spectra, and the rose color are all indicative of a LS electronic configuration.

3.1.4. 1,1,1-tris(3-methylpyrazolyl)ethane (tpe^{3Me}) and its Fe(II) complex (**3**)

While in principle tpe^{3Me} can be produced in a manner exactly analogous to tpe^{4Me} (Fig. 6), this necessitates tris(3-methylpyrazolyl)methane as a starting material. While it is a simple matter to produce regioisomeric mixtures of tpm ligands derived from 3-methylpyrazole, it has proven quite difficult to separate useful amounts of pure tris(3-methylpyrazolyl)methane from this mixture. This is not the case with the other major regioisomer, bis(3-methylpyrazolyl)(5-methylpyrazolyl)methane, which is easily crystallized from the mixture and has been the subject of a number of studies [9a,16].

As a consequence of these synthetic difficulties, an alternative route to tpe^{3Me} was devised that avoids the need for pure tris(3-methylpyrazolyl)methane. In this scheme, a regioisomeric mixture of 3-methylpyrazole tpms is methylated on the methine carbon to produce the corresponding regioisomeric mixture of tpes, which is then equilibrated in acid to produce pure tpe^{3Me} (Fig. 8). The acid-catalyzed equilibration produces close to 100% of the desired

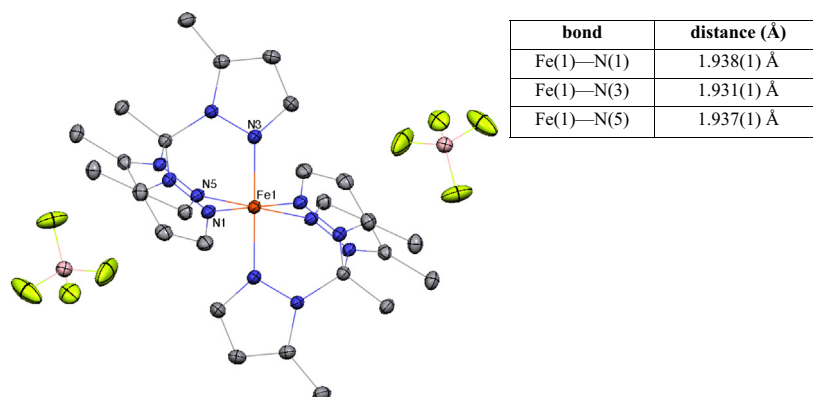


Fig. 5. Crystal structure of **5** at 100 K. Solvent molecules are not shown and hydrogen atoms have been omitted for clarity.

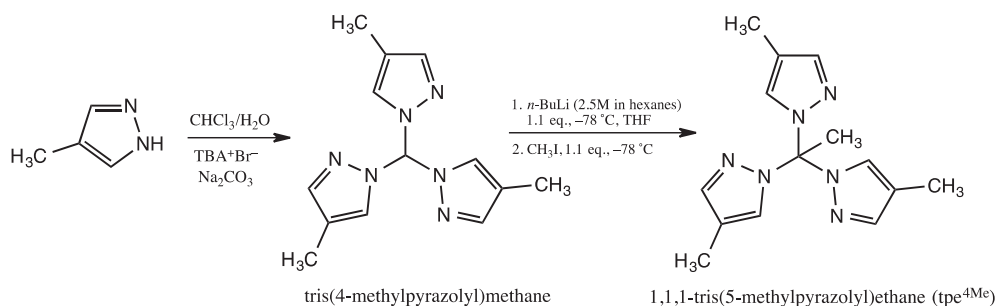


Fig. 6. Synthesis of 1,1,1-tris(4-methylpyrazolyl)ethane (tpe^{4Me}).

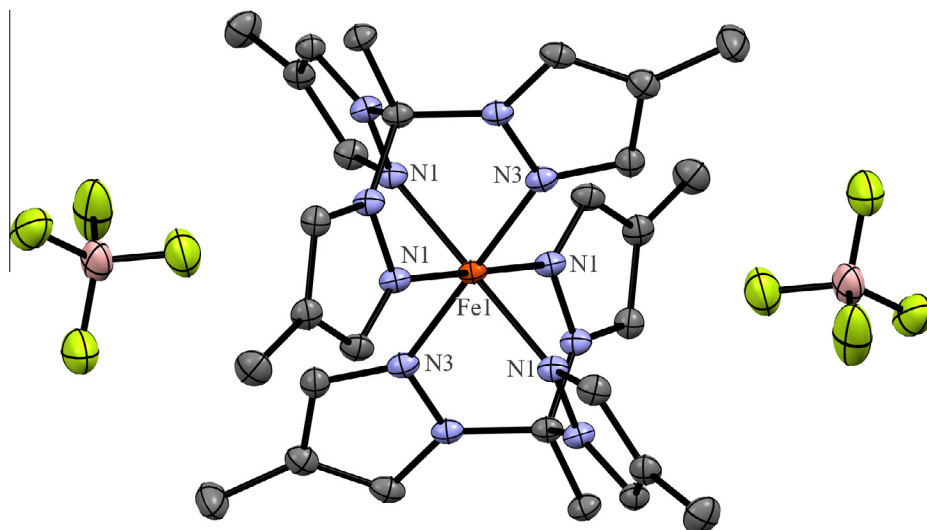


Fig. 7. Crystal structure of complex **4** at 100 K. Solvent molecules are not shown and hydrogen atoms have been omitted for clarity.

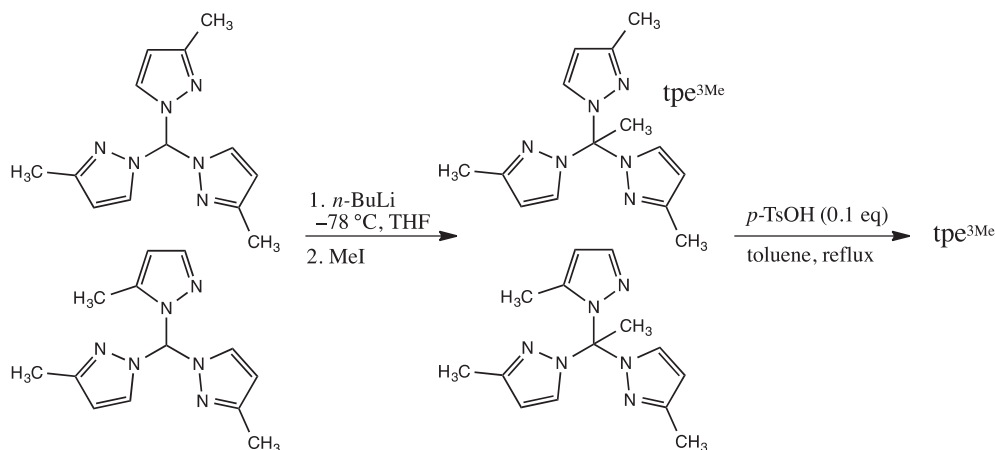


Fig. 8. The synthesis of $\text{tpe}^{3\text{Me}}$ from a regioisomeric mixture of tpm ligands.

ligand from the regioisomeric mixture, presumably due to the energetic cost of having a methyl in the 5-position of the pyrazoles in such close proximity to the methyl on the apical carbon of the tpe. The Fe(II) complex, **3** is produced in low yield by direct action of $\text{tpe}^{3\text{Me}}$ on a $\text{Fe}(\text{H}_2\text{O})_6\cdot 2\text{BF}_4$ in THF. Complex **3** is violet, as is most often encountered in simple LS Fe(II) complexes of tpm and tp ligands.

During experimental work on complex **5**, an alternative synthesis of complex **3** was discovered – **3** can be formed by thermal isomerization **5**. Simply heating an orange solution of **5** at reflux in acetonitrile for 24 h results in almost complete isomerization to **3**. Even allowing a solution of **5** to sit for extended periods at room temperature results in the slow development of purple color in the previously orange solution. The ^1H NMR spectra of the Fe(II) complex before and after heating in acetonitrile are shown in Fig. 9. A small impurity seen in the spectrum of the product **3** (peaks between 6 and 9 ppm) is believed to be the closely related Fe–tpe complex with a single methyl still remaining in the 5-position.

As can be seen in the right hand panel in Fig. 9, the ^1H NMR spectrum of **3** is quite broad and paramagnetically shifted at 25 °C. The apical methyl peak is shifted upfield to approximately $\delta = -1.0$ ppm, from a typical value (for LS tpe complexes) near

3.5 ppm. The hydrogens at C4 of the pyrazole ring are shift in the opposite direction from a typical value near 6.3 ppm to nearly 18 ppm. When these shifts are compared to those seen in other complexes of this type, the results strongly suggest the onset of SCO in solution at room temperature. Variable temperature ^1H NMR studies on **3** in acetonitrile show that the complex is essentially LS at -40 °C and conversion to HS is not nearly complete at the highest temperature studied (65 °C, see Supporting data).

X-ray crystallography was used to obtain details of the structure of **3**. The X-ray structure determined at 100 K is shown in Fig. 10. Inversion symmetry in the crystal (space group = $P\bar{1}$) once again results in three different Fe–N bond lengths, one close to 1.96 Å and the other two closer to 1.98 Å. Although longer than the Fe–N bond lengths seen for the other tpe complexes reported in this study, the bond lengths in this complex are quite typical for LS Fe(II) complexes with nitrogen donor ligands. The X-ray diffraction data collected near room temperature (293 K) shows a small but distinct lengthening of all the bonds between the ligand and the metal. Now the shortest such bond is 1.99 Å and the two longer bonds are near 2.01 Å (Fig. 10). The lengthening of the bonds is consistent with the onset of SCO to the HS electronic state in the solid state at room temperature, and agrees nicely with the solution results as determined by NMR.

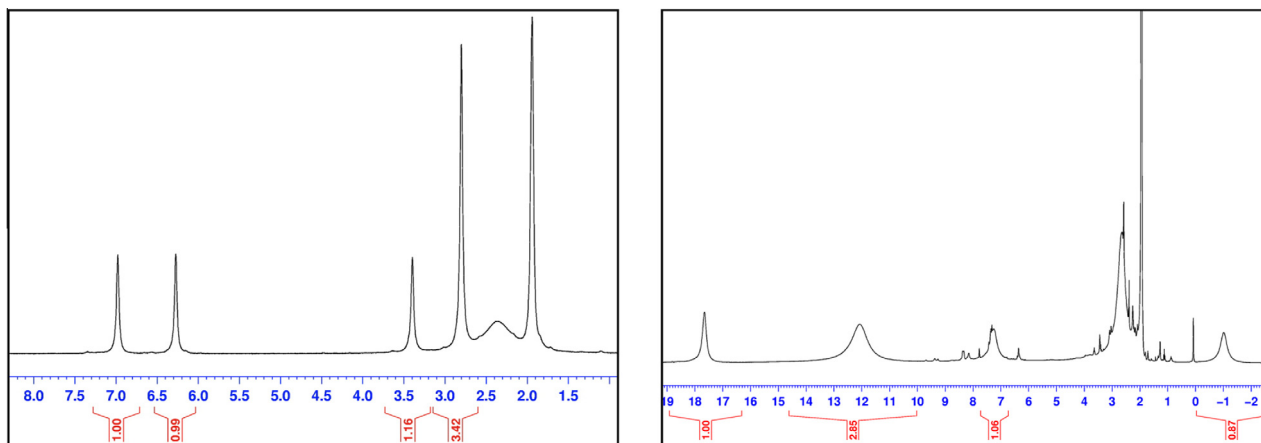


Fig. 9. The ^1H NMR spectrum of **5** (left) before heating and after heating at reflux for 24 h (right). The spectrum on the right is identical to that of **3** at 25 °C. Large signals at 1.94 and 2.4 ppm are due to CHD_2CN and H_2O , respectively.

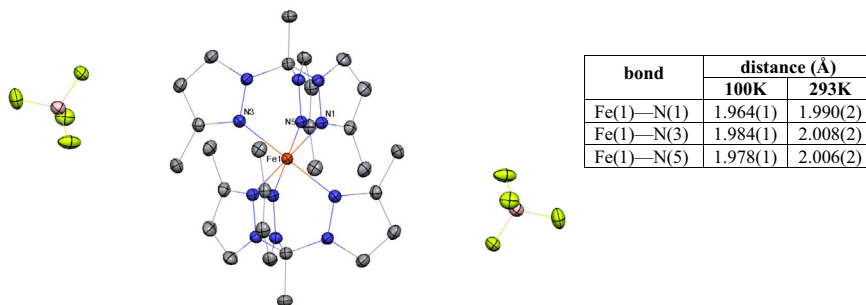


Fig. 10. Crystal structure of **3** at 100 K and Fe–N bond lengths at 100 and 293 K. Solvent molecules and hydrogen atoms are not shown.

3.2. UV–Vis spectroscopy

LS Fe(II) complexes of tpm and tp ligands are colored, typically violet. This color arises from a weak ($\epsilon \sim 100 \text{ M}^{-1} \text{ cm}^{-1}$) transition near 530 nm. All of the Fe(II)-tpe complexes synthesized in this study are colored compounds; however, three of the four complexes display colors other than violet. The Fe(II) complexes of tpe and $\text{tpe}^{4\text{Me}}$ are both rose colored and the complex of $\text{tpe}^{5\text{Me}}$ is distinctly orange. Only the complex of $\text{tpe}^{3\text{Me}}$ was the “normal” violet color typically associated with LS Fe-tpm complexes. The UV–Vis absorbance spectra of the methylated tpe complexes in acetonitrile are shown in Fig. 11. These show a distinct shift in the absorbance maximum and intensity upon moving the methyl groups around the pyrazole ring.

Since other data suggests that compound **3** is undergoing SCO, UV–Vis measurements were made on **3** to determine how the absorbance might change with temperature (see Supplementary data). The peak at $\lambda_{\text{max}} = 540 \text{ nm}$ decreases substantially ($\sim 30\%$) upon heating the sample to 65 °C, as would be expected for a compound undergoing SCO. Notably, there is also a very slight increase in absorbance between 700 and 900 nm as the temperature of **3** is increased, which is possibly due to the increase in HS complex in the solution at higher temperatures. HS complexes of this type typically show a very weak ($\epsilon \sim 1\text{--}10 \text{ M}^{-1} \text{ cm}^{-1}$) absorbance near 750 nm due to the spin-allowed, Laporte-forbidden $^5\text{T}_2 \rightarrow ^5\text{E}$ transition [17].

Diffuse reflectance measurements on solid samples of complexes **3–5** were also performed (see Supplementary data). The reflectance spectra of the three solids show trends very similar to the absorbance spectra seen in Fig. 12, but the wavelengths of least reflectance were slightly shifted when compared to the absorbance

spectra – 478 nm versus 483 nm for **5**, 510 nm versus 506 nm for **4**, and 553 nm versus 540 nm for **3**. The relative intensities of the three reflectance bands follow the same trends as the absorbance spectra, with **3** showing the least intensity and **5** exhibiting the greatest intensity.

3.3. Mössbauer spectroscopy

The Fe(II) complexes of each tpe ligand were also the subjects of a ^{57}Fe Mössbauer study. As expected for complexes **1**, **4** and **5**, the spectra showed a single transition with a very small quadrupole splitting both at low temperature and at room temperature (Table 1 and Supplementary data). These results are entirely consistent with the finding that these complexes are 100% LS, as is also indicated by X-ray, NMR, and UV–Vis data.

The Fe(II) complex **3** shows a somewhat different result (Fig. 12) than the other tpe complexes. At low temperature, **3** shows a single absorption with a small quadrupole splitting, just as for the other complexes. But at room temperature, the spectrum begins to broaden. The broadening of the line continues to 335 K. At the upper temperature limit of our Mössbauer equipment, 355 K, a distinct asymmetry begins to appear in the spectrum, which requires the use of an additional doublet for a satisfactory fit to the data. When held at higher temperatures for the prolonged periods required to obtain reasonable Mössbauer data, the compound also began show signs of rearrangement to other isomers.

4. Discussion

Unsubstituted tpe and the three methylated tpe ligands all readily form 2:1, pseudo-octahedral complexes with Fe(II), but

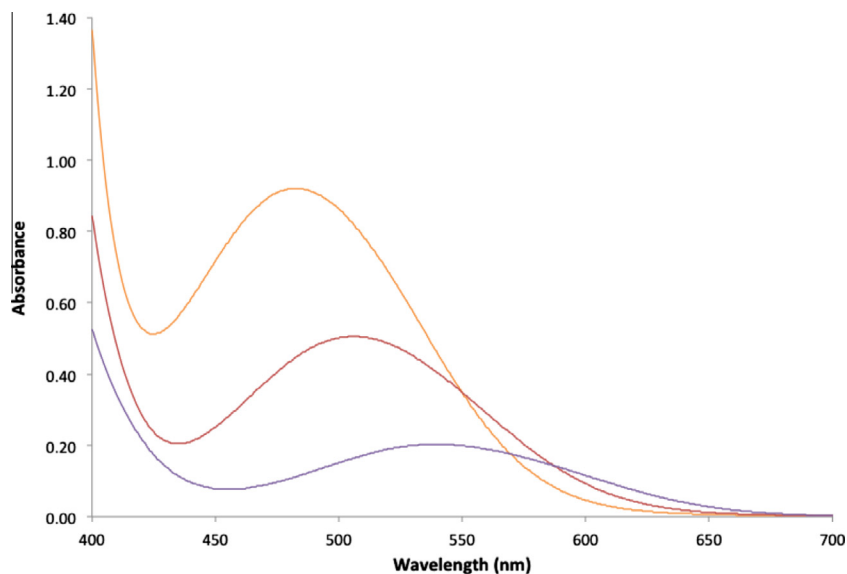


Fig. 11. The UV-Vis spectra of the Fe(II) complexes of methylated tpe ligands **3** (violet, $\lambda_{\text{max}} = 540$ nm), **4** (red, $\lambda_{\text{max}} = 506$ nm), and **5** (orange, $\lambda_{\text{max}} = 483$ nm) in acetonitrile ($c = 5$ mM). (For interpretation of the references to colour in this figure legend, the reader is referred to the web version of this article.)

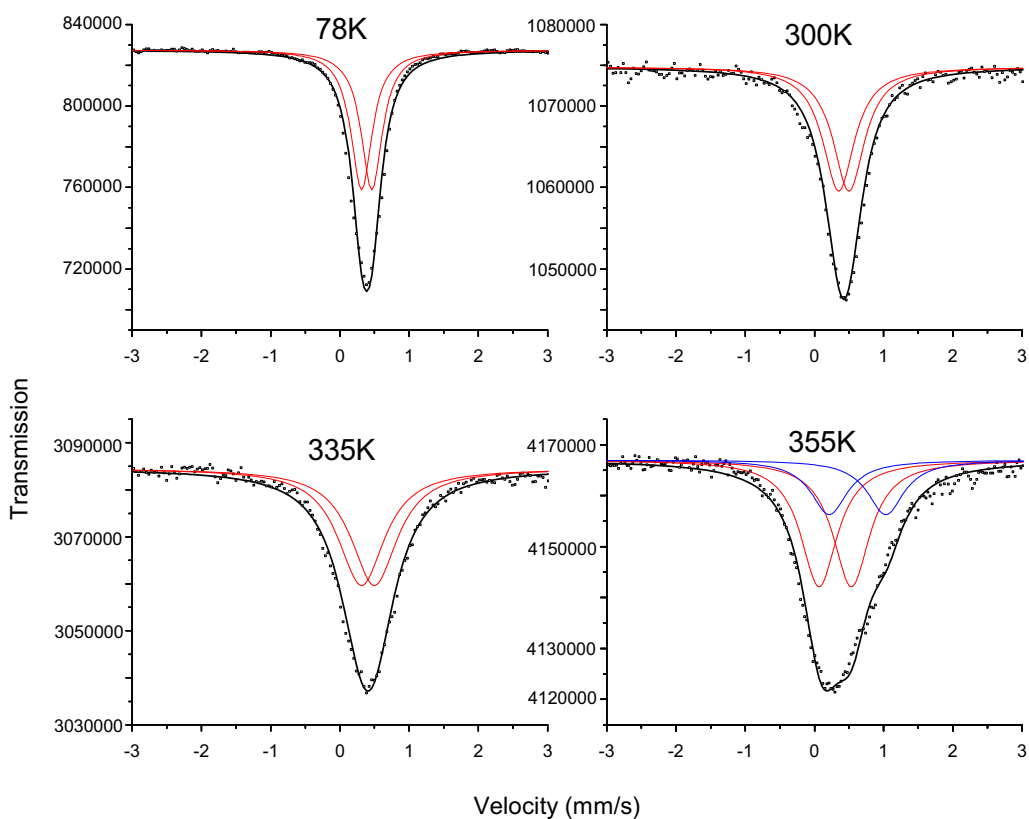


Fig. 12. The Mössbauer spectra of complex **3** at different temperatures. The data is shown fit with a doublet (red) at lower temperatures, but requires additional lines at 355 K (blue). (For interpretation of the references to colour in this figure legend, the reader is referred to the web version of this article.)

with somewhat different structural details. These differences give direct insight into the effect of methylating the pyrazoles at different positions of a tpm-like ligand when a methyl is also present on the methine carbon. The Fe(II) complex of the unsubstituted tpe can be appropriately compared to the analogous complex of the unsubstituted tpm [14a]. Both are LS at room temperature in solution and in the solid state. However, the tpm complex is violet and

just beginning to show signs of SCO behavior at room temperature, whereas the tpe complex is rose colored and shows no tendency towards a changeover to HS. This simple comparison strongly suggests that the interaction of the methyl group of tpe with the hydrogens in the 5-position of the pyrazoles is forcing the “bite” of the ligand closed. This is entirely consistent with the fact that the Fe–N bond lengths of tpe complex **1** are also shorter than those

Table 1
⁵⁷Fe Mössbauer parameters for the Fe(II) complexes in this study.

| Complex | T (K) | IS (mm/s) | QS (mm/s) |
|----------|-------|-----------|-----------|
| 1 | 78 | 0.32 | 0.30 |
| | 300 | 0.36 | 0.28 |
| 3 | 78 | 0.42 | 0.15 |
| | 300 | 0.42 | 0.15 |
| 4 | 78 | 0.31 | 0.29 |
| | 300 | 0.36 | 0.32 |
| 5 | 78 | 0.24 | 0.34 |
| | 300 | 0.31 | 0.38 |

in the analogous tpm complex (1.95 Å as compared to 1.97 Å). The shorter Fe–N bonds in complex **1** result in a stronger ligand field than the related tpm complex, which has the dual affect of increasing the energy of the ¹A₁ → ¹T₁ transition (λ_{\max} 505 nm versus 535 nm) [17] and destabilizing the HS complex relative to the LS form.

Substitution in the 4-position of the pyrazole (tpe^{4Me}) has very little affect on the electronic and bonding properties of the Fe(II) complex **4** as compared to the unsubstituted tpe complex **1**. The Fe(II) complexes **1** and **4** are both LS and rose colored (λ_{\max} 505 nm vs. 506 nm). Each complex also has Fe–N bonds averaging about 1.95 Å long. A similar conclusion can be drawn when comparing the analogous tpm complexes to each other; the complexes of tris(4-methylpyrazolyl)methane and those of unsubstituted tpm also share similar properties [18]. This is not surprising, since substituents in the 4-position of the pyrazoles are situated so that they point directly away from the core of the complex, so they do not interact strongly with the either the methine substituent or with substituents on the second ligand.

In previous work [8], substituents in the 5-position of tpm complexes have been shown to close the bite of the ligand, increasing the ligand field splitting and therefore stabilizing the LS state relative to the HS state. In the present study, the effect of substitution in the 5-position (tpe^{5Me}) is magnified due to the presence of a methyl group on the methine carbon of the tpe. Upon formation of the metal complex, the three methyl groups of the pyrazoles are forced into very close proximity to the methine methyl group. It is expected that the structural changes associated with a transition to HS state, primarily lengthening of the Fe–N bonds, would force these methyls even closer together, so the complex is firmly entrenched in the LS state. The close proximity of the methyls leads to other features which make the Fe(II) complex **5** stand out from the others in the series under study. First, the Fe(II) complex is an unexpected color, orange, with a λ_{\max} of 483 nm. This indicates that Δ_{Oct} is larger for this than any of the other tpe complexes investigated. Second, the metal complex rearranges almost completely to the presumably less-hindered **3** over time in solution at room temperature, and much more rapidly if heated. This suggests that the energetic cost of placing groups in the 5-position, where they are crowded by the tpe methyl, is higher than placing them in the 3-position, where they incur energy costs from interligand repulsions.

All together, the evidence paints a picture of [Fe(tpe^{5Me})₂]²⁺ as an ion with severe steric problems, which is confirmed by a close inspection of the X-ray structure. The carbon atoms on the 5-positions are located only 2.95 Å from the carbon of the methine methyl, significantly closer than the sum of the van der Waals radii of two carbon atoms (3.40 Å). These are unusually short intramolecular contact distances for methyl groups [19], but are unavoidable if the ligand is to form a tripodal metal complex with its inherent rigidity. The molecular structure shows clear signs of strain from these close CH₃ ··· CH₃ interactions. The bond between the 5-methyl and the carbon of the pyrazole is bent away from the methine methyl – the N–C–CH₃ bond angles average just over

129°. In the analogous tpm complex, the N–C–CH₃ bond angles range from 121.5° to 123.2° (3 structures with different anions). Also, the steric repulsion between the methyls has apparently closed the bite of the ligand and thus shortened the Fe–N bonds to the shortest observed so far in tpm-type complexes, 1.931–1.938 Å. The overall structure is also more trigonally distorted away from octahedral geometry – the intra-ligand N–Fe–N angles in **5** average 86.6° in the solid state, whereas those for **4** average 87.2° and for **3** are 88.1°. Finally, the fact that **5** rearranges in solution to **3** confirms that given the choice, the methyl groups are more stable in the 3-position of a tpe when in an octahedral complex. A somewhat analogous rearrangement was observed by Trofimenko for Co(II) complexes of tp with isopropyl groups in the 3-position of the pyrazoles, but in this case one of the pyrazoles rearranged to the 5-position to relieve interligand repulsions [20].

The Fe(II) complex **3** is the usual purple color, with λ_{\max} = 540 nm. The Fe–N bond distances are also more “typical” for LS Fe-tpm complexes, 1.964–1.984 Å. Unlike tpe^{4Me} and tpe^{5Me}, the pyrazole-methyls in tpe^{3Me} are oriented towards the second ligand when it is in octahedral complex **3**. The effects of substituents in the 3-position of tpm and tp complexes have been well studied [18,21]. These substituents, if small enough to allow for 2:1 complex formation, tend to open the bite of the ligand and therefore lengthen (and weaken) the Fe–N bonds. The weakened ligand field then begins to favor the HS electron configuration for the complex at room temperature. Calculations suggest that the weakening of the Fe–N bonds is the direct result of repulsion between groups in the 3-position as they are forced too close to the second ligand when forming a 2:1 complex with the metal. When compared to **1** and **4**, the properties of **3** are best understood in terms of the crowding of the methyl groups in the 3-position being opposed by the bite-closing effect of the methyl on the methine carbon. The results suggest that the interligand repulsion of 3-methyls is almost completely mitigated by the intraligand repulsion between the methine methyl and the hydrogens in the 5-position of the pyrazoles. The balancing of these two opposing effects in **3** results in a value of Δ_{Oct} that is low enough to allow SCO, albeit at temperatures above room temperature, and in this respect it is similar to the completely unsubstituted Fe-tpm and Fe-tp complexes. Onset of SCO in solution is clearly evident in the ¹H NMR spectrum and the UV–Vis data, and both the X-ray and the Mössbauer measurements support the onset of SCO in the solid. To our knowledge, this is the first example of a methine-substituted tpm complex of Fe(II) showing any sign of SCO behavior.

Mössbauer parameters for all the new tpe complexes were measured at low temperature and room temperature. At 78 K, all of the tpe complexes have isomer shift (IS) values in the expected range for LS Fe(II) complexes of this type. Values of the quadrupole splitting (QS) are quite small, 0.02–0.03, and typical for this class of LS compounds (see Supplementary data). For octahedral Fe(II) complexes in the ¹A_{1g} state one expects zero quadrupole splitting. However, the octahedral symmetry is distorted by elongation along the three-fold rotational axis passing through the central Fe atom and the two bridging carbon atoms at opposite sides of the complex moiety. As a result of the trigonal distortion, the angle between three-fold, D₃ axis and the Fe–N bonds are smaller than the ‘magic’ angle (54.74°) present in an ideal octahedron and quadrupole splitting can be observed [22]. Using a simple geometrical model, QS can be expressed as:

$$QS = 6 \times (3 \cos^2 \theta - 1) \times PQS$$

where PQS are partial quadrupole splitting constants for given donor groups. Taking into account the experimental angles θ , which are 52.7–52.8° for compounds **1** and **4**, 52.3–52.6° for **5** and 53.3–53.4° for **3** and using 0.5 as a basic estimate for PQS for the pyrazole

donors in the tpe ligands (values for various ligands with aromatic N-donor atoms vary from 0.4 to 0.6 [22b]), QS can be estimated to be 0.27 for **1** and **4**, 0.32 for **5** and 0.19 for **3**. These values are in reasonable qualitative agreement with the experimental data (see Supplementary).

Both the IS and QS values of **1**, **4**, and **5** undergo only small changes with temperature from 78 to 300 K, and the peak widths also change only slightly. In contrast, complex **3** displays different behavior. In this case, while the 78 K spectrum is similar to the other tpe complexes, a slight but noticeable broadening occurs by 300 K. The broadening of the line continues as the temperature is raised to 335 K. At the highest temperature investigated, 355 K, the spectrum of **3** becomes distinctly asymmetric with a slight shoulder beginning to appear near an IS of 1.0 mm/s. The onset of broadening in the Mossbauer spectrum of **3** at 300 K corresponds with lengthening of the Fe–N bonds in the X-ray structure and the broadening and shifting of ^1H NMR signals in solution, which suggests that this effect is due to the onset of SCO. Similar features in the Mössbauer spectra of $[\text{Fe}(\text{tpm})_2](\text{BF}_4)_2$ and $[\text{Fe}(\text{tpm})_2](\text{PF}_6)_2$ have been interpreted as the result of a dynamic LS/HS spin-equilibrium occurring on the timescale of the Mössbauer measurement [14a,23]. The lack of a clearly distinct set of new lines with a much larger splitting as the temperature is raised, which might be expected for the HS form of **3**, is therefore due to the low activation energy and rapid rate of the spin equilibrium being observed. While it is not possible to quantitate the SCO process using the data we obtained, qualitatively the result demonstrates that complex **3** is undergoing SCO in the solid state at room temperature.

The Fe(II)-tpe complexes all display a weak, spin-allowed (but Laporte-forbidden) $d-d$ transition in the visible spectrum, which is the origin of their various colors [17]. Two similar transitions are expected for LS octahedral d_6 complexes, but only one is actually observed in the present complexes. The observed transition is probably the lower energy transition ($^1A_{1g} \rightarrow ^1T_{1g}$), with the unobserved higher energy transition ($^1A_1 \rightarrow ^1T_2$) likely obscured by a MLCT band near 330 nm. The absorbance spectra combined with the Fe–N bond lengths of the various Fe-tpe complexes show that the location of the methyl group on the periphery of the pyrazole directly affects the strength of the ligand field on the metal and therefore the transition energies between d orbitals of the iron. Moreover, the energy of this transition can give some insight into the energy required for a given SCO transition in Fe-tris(pyrazolyl) complexes. As is evident from the Tanabe–Sugano diagram for d^6 octahedral complexes, the energy difference between the 1A_1 ground state (LS) and the 5T_2 excited state (HS) increases more rapidly than the energy of the $^1A_1 \rightarrow ^1T_1$ transition as the ligand field strength (Δ_{oct}) is increased. Thus, it is reasonable to comment on the likelihood of a SCO transition in a LS Fe-tpm complex simply by measuring the UV–Vis spectrum of the complex, or even by just noting its color. To date, only those complexes with λ_{max} near 530 nm, which are violet, have shown any tendency to undergo a spin transition. This value of λ_{max} suggests that Δ_{oct} is small enough to also allow for the possibility of a thermal transition between the 1A_1 and the 5T_2 state (SCO). Assuming that the Racah B parameters for all Fe-tpm and -tpe complexes are relatively similar, those complexes that display spectroscopic transitions at wavelengths significantly below 530 nm and therefore appear rose or even orange colored, have little chance of having an observable spin transition up to room temperature, or even well above room temperature, as their ligand fields are simply too strong and the energy differences between the LS and HS state is too great to be accessed thermally. Solid-state spectra measured by diffuse reflectance can also be used to make this qualitative judgment.

Finally, it is noted that the strength of the visible absorption band decreases noticeably on going from **3** ($\epsilon = 40 \text{ cm}^{-1} \text{ M}^{-1}$) to **4**

($\epsilon = 100 \text{ cm}^{-1} \text{ M}^{-1}$) to **5** ($\epsilon = 200 \text{ cm}^{-1} \text{ M}^{-1}$). While some of the weakness in the measured $[\text{Fe}(\text{tpe}^{3\text{Me}})_2]^{2+}$ band can be attributed to the gradual changeover to HS that has already begun in solution at room temperature, the NMR and X-ray evidence suggests that SCO in **3** is only 10–20% complete at room temperature, which is clearly insufficient to account for the intensity of the band. SCO also explains nothing in regards to the relative magnitude of the visible band of complex **4** when compared to complex **5**, since these are both 100% LS in solution at room temperature. The best explanation for the observed trend is therefore probably intensity borrowing [17], whereby Laporte-forbidden $d-d$ bands are generally more intense as their energy nears allowed transitions involving orbitals with p -character (ungerade). In the present case, there is a large ($\epsilon \sim 7000 \text{ cm}^{-1} \text{ M}^{-1}$) MLCT band near 330–340 nm in each LS tpe complex, the tail end of which is visible in Fig. 11, which provides the necessary conditions for this phenomenon. The closer the $d-d$ transition is to the energy of this band, the more strongly the bands are coupled and the more intense the $d-d$ transition becomes.

5. Conclusion

Four tris(pyrazolyl)ethane (tpe) ligands (tpe, $\text{tpe}^{3\text{Me}}$, $\text{tpe}^{4\text{Me}}$, and $\text{tpe}^{5\text{Me}}$), differing only in placement of methyl groups on the pyrazole rings have been successfully synthesized and characterized. In each case the 2:1 complex with Fe(II) was readily synthesized. The complexes were all low spin, but differed in Fe–N bond lengths and color. Methyls in the 5-position of the tpe ($\text{tpe}^{5\text{Me}}$) closed the bite of the ligand, strengthening the ligand field and shifting the visible absorbance band to higher energies. Methyls in the 4-position ($\text{tpe}^{4\text{Me}}$) had almost no effect on the ligand, making it quite comparable to the unsubstituted tpe ligand. Methyls in the 3-position ($\text{tpe}^{3\text{Me}}$) cause an opening of the bite of the ligand, which is evidenced by increased Fe–N bond lengths and a shift of the visible absorbance to lower energies. This explains why the Fe(II) complex of $\text{tpe}^{3\text{Me}}$ is beginning to display spin crossover behavior near room temperature.

Acknowledgements

Financial support for this project was provided by Faculty Research Council, D'Youville College. M.J.D. and S.E.T. gratefully acknowledge the U.S. DOE Grant, No. DEFG02-03ER46064 for support of their Mössbauer work. M.J.D. also appreciatively thanks Prof. Gary Pettibone for his persistent commentary and critiques. M.S.G. thanks Prof. William S. Durfee for helpful discussions related to the writing of portions of this manuscript.

Appendix A. Supplementary material

CCDC 1005976–1005980 contains the supplementary crystallographic data for this paper. These data can be obtained free of charge from The Cambridge Crystallographic Data Centre via www.ccdc.cam.ac.uk/data_request/cif. Supplementary data associated with this article can be found, in the online version, at <http://dx.doi.org/10.1016/j.ica.2014.08.046>.

References

- [1] (a) J.P. Jesson, S. Trofimenko, D.R. Eaton, J. Am. Chem. Soc. 89 (3148) (1967) 1970, <http://dx.doi.org/10.1021/ja00989a014>;
(b) S. Trofimenko, J. Am. Chem. Soc. 92 (1970) 5118, <http://dx.doi.org/10.1021/ja00720a021>.
- [2] (a) C. Santini, M. Pelli, G.G. Lobbia, G. Papini, Mini-Rev. Org. Chem. 7 (2) (2010) 84, <http://dx.doi.org/10.2174/157019310791065519>;
(b) H.R. Bigmore, S.C. Lawrence, P. Mountford, C.S. Tredget, Dalton Trans. 4 (2005) 635, <http://dx.doi.org/10.1039/B413121E>;

- (c) S. Trofimenko, *Scorpionates: The Coordination Chemistry of Polypyrazolylborate Ligands*, Imperial College Press, River Edge, NJ, 1999;
- (d) D.L. Reger, *Comments Inorg. Chem.* 21 (1–3) (1999) 1, <http://dx.doi.org/10.1080/02603599908020413>;
- (e) C. Pettinari, R. Pettinari, *Coord. Chem. Rev.* 249 (2005) 525, <http://dx.doi.org/10.1016/j.ccr.2004.05.010>;
- (f) C. Pettinari, *Scorpionates II: Chelating Borate Ligands*, Imperial College Press, London, 2008;
- (g) G.J. Long, F. Grandjean, D.L. Reger, in: P. Gülich, H.A. Goodwin (Eds.), *Spin Crossover in Transition Metal Compounds, Part I. Topics in Current Chemistry*, vol. 233, Springer-Verlag, Berlin, 2004, p. 91, <http://dx.doi.org/10.1007/b13530>.
- [3] (a) O. Kahn, C.J. Martinez, *Science* 279 (44) (1998) 1994, <http://dx.doi.org/10.1126/science.279.5347.44>;
- (b) P. Gülich, A. Hauser, H. Spiering, *Angew. Chem., Int. Ed. Engl.* 33 (2003) 2024, <http://dx.doi.org/10.1002/anie.199420241>.
- [4] (a) J. Kröber, E. Codjovi, O. Kahn, F. Grolière, C. Jay, *J. Am. Chem. Soc.* 115 (9810) (1993) 1994, <http://dx.doi.org/10.1021/ja00074a062>;
- (b) J. Kröber, J.-P. Audière, E. Codjovi, O. Kahn, J.G. Haasnoot, F. Grolière, C. Jay, A. Bousseksou, J. Linares, F. Varret, A. Gonthier-Vassal, *Chem. Mater* 6 (1994) 1404, <http://dx.doi.org/10.1021/cm00044a044>;
- (c) Y. Garcia, P.J. van Koningsbruggen, R. Lapouyade, L. Fournès, L. Rabardel, O. Kahn, V. Ksenofontov, G. Levchenko, P. Gülich, *Chem. Mater.* 10 (1998) 2426, <http://dx.doi.org/10.1021/cm980107>;
- (d) O. Roubeau, J.M. Alcazar Gomez, E. Balskus, J.J.A. Kolnaar, J.G. Haasnoot, J. Reedijk, *J. New Chem.* 25 (2001) 144, <http://dx.doi.org/10.1039/B007094G>.
- [5] (a) D.L. Reger, T.C. Grattan, *Synthesis* 3 (350) (2003) 1989, <http://dx.doi.org/10.1055/s-2003-37339>;
- (b) M.A. Esteruelas, L.A. Oro, R.M. Claramunt, C. Lopez, J.L. Lavandera, J. Elguero, *J. Organomet. Chem.* 366 (1989) 245, [http://dx.doi.org/10.1016/0022-328X\(89\)87330-9](http://dx.doi.org/10.1016/0022-328X(89)87330-9);
- (c) A.R. Katritzky, A.E. Abdel-Rahman, D.E. Leahy, O.A. Schwarz, *Tetrahedron* 39 (1983) 4133, [http://dx.doi.org/10.1016/S0040-4020\(01\)88633-6](http://dx.doi.org/10.1016/S0040-4020(01)88633-6);
- (d) E. Diez-Barra, A. de la Hoz, A. Sanchez-Migallon, J. Tejada, *J. Chem. Soc., Perkin Trans. 1* (1993) 1079, <http://dx.doi.org/10.1039/P19930001079>;
- (e) R. Wanke, P. Smolenski, M.F.C.G. da Silva, *Inorg. Chem.* 47 (2008) 10158, <http://dx.doi.org/10.1021/ic801254b>;
- (f) P.K. Byers, A.J. Canty, R.T. Honeyman, R.M. Claramunt, C. Lopez, J.L. Lavandera, J. Elguero, *Gazz. Chim. Ital.* 122 (1992) 344.
- [6] I. Garcia-Orozco, R. Quijada, K. Vera, M. Valderrama, *J. Mol. Catal. A: Chem.* 260 (1–2) (2006) 70, <http://dx.doi.org/10.1016/j.molcata.2006.06.048>.
- [7] (a) L.D. Reger, E. Sirianni, J.J. Horger, M.D. Smith, *Cryst. Growth Design* 10 (386) (2010) 2009, <http://dx.doi.org/10.1021/cg901000d>;
- (b) D.L. Reger, C.A. Little, R.F. Semeniuc, M.D. Smith, *Inorg. Chim. Acta* 362 (2009) 303, <http://dx.doi.org/10.1016/j.ica.2008.03.120>.
- [8] M.A. Goodman, A.Y. Nazarenko, B.J. Casavant, Z. Li, W.W. Brennessel, M.J. DeMarco, G. Long, M.S. Goodman, *Inorg. Chem.* 51 (2) (2012) 1084, <http://dx.doi.org/10.1021/ic2022038>.
- [9] (a) C. Pettinari, M. Pellei, A. Cingolani, D. Martini, A. Drozdov, S. Troyanov, W. Panzeri, A. Mele, *Inorg. Chem.* 38 (5777) (1999) 2000, <http://dx.doi.org/10.1021/ic9906252>;
- (b) D.L. Reger, T.C. Grattan, K.J. Brown, C.A. Little, J.J.S. Lamba, A.L. Rheingold, R.D. Sommer, *J. Organomet. Chem.* 607 (2000) 120, [http://dx.doi.org/10.1016/S0022-328X\(00\)00290-4](http://dx.doi.org/10.1016/S0022-328X(00)00290-4).
- [10] G.M. Sheldrick, *SADABS, Version 2007/4*, University of Göttingen, Göttingen, Germany, 2007.
- [11] A. Altomare, M.C. Burla, M. Camalli, G.L. Cascarano, C. Giacovazzo, A. Guagliardi, A.G.G. Moliterni, G. Polidori, R. Spagna, *SIR97: A New Program for Solving and Refining Crystal Structures*, Istituto di Cristallografia, CNR, Bari, Italy, 1999.
- [12] G.M. Sheldrick, *Acta. Crystallogr., Sect. A* 64 (2008) 112, <http://dx.doi.org/10.1107/S0108767307043930>.
- [13] G. Long, M. DeMarco, M. Chudyk, J. Steiner, D. Coffey, H. Zeng, Y.K. Li, G.H. Cao, Z.A. Xu, *Phys. Rev. B* 84 (2011) 064423, <http://dx.doi.org/10.1103/PhysRevB.84.064423>.
- [14] (a) D.L. Reger, C.A. Little, A.L. Rheingold, M. Lam, L.M. Liabe-Sands, B. Rhagitan, T. Concolino, A. Mohan, G.J. Long, V. Briois, F. Grandjean, *Inorg. Chem.* 40 (1508) (2001) 2001, <http://dx.doi.org/10.1021/ic001102t>;
- (b) V. Briois, P. Sainctavit, G.J. Long, F. Grandjean, *Inorg. Chem.* 40 (2001) 912, <http://dx.doi.org/10.1021/ic0007153>.
- [15] (a) M.G. Cushion, J. Meyer, A. Heath, A.D. Schwarz, I. Fern, F. Breher, P. Mountford, *Organometallics* 29 (1174) (2010) 2009, <http://dx.doi.org/10.1021/om901013b>;
- (b) I. Fernandez, P.O. Burgos, F. Armbruster, I. Krummenacher, F. Breher, *Chem. Commun.* 18 (2009) 2586, <http://dx.doi.org/10.1039/b902053e>;
- (c) H.R. Bigmore, J. Meter, I. Krummenacher, H. Ruegger, E. Clot, P. Mountford, F. Breher, *Chem. Eur. J.* 14 (19) (2008) 5918, <http://dx.doi.org/10.1002/chem.200800181>.
- [16] (a) D. Martini, M. Pellei, C. Pettinari, B.W. Skelton, A.H. White, *Inorg. Chim. Acta* 333 (72) (2002) 2009, [http://dx.doi.org/10.1016/S0020-1693\(02\)00772-7](http://dx.doi.org/10.1016/S0020-1693(02)00772-7);
- (b) D.L. Reger, J.D. Elgin, E.A. Foley, M.D. Smith, F. Grandjean, G. Long, *J. Inorg. Chem.* 48 (2009) 9393, <http://dx.doi.org/10.1021/jc901259e>.
- [17] J.P. Jesson, S. Trofimenko, D.R. Eaton, *J. Am. Chem. Soc.* 89 (1967) 3158, <http://dx.doi.org/10.1021/ja00989a015>.
- [18] H. Paulsen, L. Duellund, A. Zimmermann, F. Averseng, M. Gerdan, H. Winkler, H. Toftlund, A.X. Trautwein, *Monatsh. Chem.* 134 (2003) 295, <http://dx.doi.org/10.1007/s00706-002-0522-7>.
- [19] R. Taylor, *J. Chem. Inf. Model.* 51 (2011) 897, <http://dx.doi.org/10.1021/ci100466h>.
- [20] S. Trofimenko, J.C. Calabrese, P.J. Domaille, J.S. Thompson, *Inorg. Chem.* 28 (1989) 1091, <http://dx.doi.org/10.1021/ic00305a019>.
- [21] M. Güell, M. Solà, M. Swart, *Polyhedron* 29 (2010) 84, <http://dx.doi.org/10.1016/j.poly.2009.06.006>.
- [22] (a) W.M. Reiff, *J. Am. Chem. Soc.* 95 (3048) (1973) 2002, <http://dx.doi.org/10.1021/ja00790a071>;
- (b) Y.Z. Voloshin, E.V. Polshin, A.Y. Nazarenko, *Hyperfine Interact.* 141/142 (2002) 309, <http://dx.doi.org/10.1023/A:1021215817257>.
- [23] H. Winkler, A.X. Trautwein, H. Toftlund, *Hyperfine Interact.* 70 (1–4) (1992) 1083, <http://dx.doi.org/10.1007/BF02397517>.